Title: Machine learning reveals the effect of leaf temperature extremes on shifts in plant photosystem heat tolerance thresholds

Author names: Catherine Pottinger[1], Pieter A. Arnold[2], Michelle Bird[1], Lisa M. Danzey[1], Sonya R. Geange[3,4], Andrei Herdean[5], Adrienne B. Nicotra[2], Andy Leigh[1]

Affiliations:

[1]University of Technology Sydney, School of Life Sciences, Broadway, NSW 2007, Australia.

[2] Division of Ecology and Evolution, Research School of Biology, The Australian National University, Canberra, ACT 2600 Australia.

[3]University of Bergen, Department of Biological Sciences, Bergen, 5008 Norway.

[4]Bjerknes Centre for Climate Research, University of Bergen, Norway

[5]University of Technology Sydney, Climate Change Cluster, Broadway, NSW 2007, Australia.

Catherine Pottinger (corresponding author): https://orcid.org/0009-0001-2436-5069

catie.a.pottinger@student.uts.edu.au

Pieter Arnold: https://orcid.org/0000-0002-6158-7752

Lisa Danzey: https://orcid.org/0009-0005-0314-9075

Sonya Geange: https://orcid.org/0000-0001-5344-7234

Andrei Herdean: https://orcid.org/0000-0003-2143-0213

Adrienne Nicotra: https://orcid.org/0000-0001-6578-369X

Andy Leigh: https://orcid.org/0000-0003-3568-2606

Funding

Australian Research Council Linkage Projects grant LP180100942, held by AN and AL; Australian Government Research Training Program Scholarship, held by CP.

Conflicts of Interest

The authors declare no conflicts of interest.

Data availability

If accepted for publication, data will be made available on Dryad and the code used for analyses, on GitHub.

Keywords

Heat tolerance, leaf temperature, microclimate, alpine, T_{crit}, cross tolerance, extreme temperatures

Abstract

Plant physiological heat tolerance thresholds can acclimate rapidly in response to changing leaf temperature, which varies considerably across microclimatic space and time. How leaf temperatures trigger shifts in these heat thresholds has not been established. We aimed to determine the influence of temporally proximal leaf temperatures (T^{leaf}) on leaf photosystem heat tolerance thresholds (T_{crit}) for two co-occurring plant species *in situ* in the Australian Alps. We measured T_{crit} and T^{leaf} over five days at 16 sites, paired by aspect (northwest, southeast) across two locations: a cold air drainage valley and a high exposed ridgeline. To investigate how T_{crit} was influenced by T^{leaf} in the days prior, we used traditional statistical approaches (linear mixed models) and a machine learning technique. While traditional models found that T^{leaf} parameters explained some variation in T_{crit}, machine learning identified that 85% of the variation in T_{crit} was explained by both maximum and minimum leaf temperatures in the four days prior to measurement. This finding illustrates that heat tolerance acclimation is driven by exposure to not only maximum, but also minimum leaf temperatures. To uncover complex relationships between fluctuating environmental conditions and plant acclimatory responses, we recommend integrating machine learning techniques with traditional statistical methods.

Introduction

Many of the critical physiological processes of plants, including photosynthesis, tissue repair and reproduction, are mediated by temperature (Wahid et al. 2007). Ascertaining the thermal limits to physiological function, or thermal tolerance thresholds, and how they shift with local temperature, is critical if plant vulnerability to climatic warming is to be characterised accurately (Cook et al. 2021). It is becoming increasingly clear that coarse gradient measures of climate do not predict significant variation in heat tolerance thresholds at a local scale (Curtis et al. 2016, Feeley et al. 2020, Perez and Feeley 2020, Danzey et al. 2024). Indeed, in common garden settings, differences in heat tolerance thresholds are reduced relative to *in situ* measurements (Knight and Ackerly 2002, Knight and Ackerly 2003, Harris et al. 2024, Alvarez et al. 2025), indicating acclimation to local conditions. Heat tolerance acclimation in plants broadly refers to the reversible physiological and morphological adjustments that enable plants to modify their thermal limits in according to prevailing environmental conditions (Wahid et al. 2007, Zhu et al. 2018). Further, leaf temperatures can strongly decouple from air, exceeding air temperatures by >10°C under hot conditions (Körner and Cochrane 1983, Blonder and Michaletz 2018, Fauset et al. 2018); the extent of this decoupling is mediated by morphological traits that influence leaf thermodynamics (Leigh et al. 2017, Arnold et al. 2025a). For these reasons, focus has shifted toward the influence of leaf temperature on thermal tolerance, particularly photosystem heat tolerance (Perez and Feeley 2020, Cook et al. 2021, Zhu et al. 2024). There is evidence to suggest that microclimate, through its influence on leaf temperatures, is a strong predictor of heat tolerance thresholds (Buchner and Neuner 2003, Curtis et al. 2016, Leon-Garcia and Lasso 2019). This association is particularly important to investigate in places typified by high microclimatic heterogeneity and temporal variability, such as alpine environments (Körner 2003, Körner and Hiltbrunner 2021, Körner 2023).

Average temperatures do not necessarily capture the extremes to which plants are exposed. Nor do they account for the influence of heat load, a function of temperature intensity and exposure duration, on heat tolerance (Neuner and Buchner 2023, Cook et al. 2024, Faber et al. 2024). While climate change is bringing warmer daytime temperatures, nighttime temperatures may be increasing at a greater rate (Easterling et al. 1997, Donat and Alexander 2012), which has implications on important aspects of plant physiology and

reproduction (Willits and Peet 1998, Niu and Xiang 2018, Rahnama et al. 2024). Among these physiological processes, PSII acclimation is particularly important, as it reflects the ability of the photosynthetic apparatus to maintain function under increasingly stressful thermal conditions. This phenomenon has been observed as changes in PSII heat tolerance thresholds (Posch et al. 2022, Sumner et al. 2022, Andrew et al. 2023, Cook et al. 2024, Danzey et al. 2024). Research on heat tolerance thresholds typically focuses on the effect of increasing or maximum temperatures (Leon-Garcia and Lasso 2019, Perez and Feeley 2020, Vilas-Boas et al. 2024), while the effect of minimum temperatures has received far less attention. Further, diurnal temperature amplitude can exert a substantial effect on drought and freezing tolerance (Zhang et al. 2023). However, the effect of temperature across diurnal cycles on heat tolerance thresholds under natural conditions remains to be studied. Regarding the effect of temperature history on heat tolerance, some authors suggest that acclimation is influenced by mean and maximum daily temperatures in the days prior to measurement (Hüve et al. 2006, Curtis 2017, Bison and Michaletz 2024, Zhu et al. 2024). Conversely, others have found that acclimation of heat thresholds occurs over longer temporal scales, across months and seasons (Zhu et al. 2018, Leon-Garcia and Lasso 2019). It remains unclear as to what temporal scale acclimation of these thresholds occurs across and the magnitude of the cues that trigger threshold shifts.

The thermal triggers for heat tolerance acclimation are complex. Relationships between heat tolerance and temperature are not linear, with discrepancies between threshold relaxation and leaf temperature documented in alpine environments (Buchner and Neuner 2003, Neuner and Buchner 2012). Therefore, traditional statistical methods that rely on average temperatures to predict heat tolerance present clear limitations, particularly for data collected under field conditions, where environmental temperatures vary across microclimates and plants are exposed to rapid temperature fluctuations. Predicting thermal tolerance necessitates a more nuanced assessment of how temporally proximal temperatures lead to shifts in heat tolerance thresholds. Machine learning has recently been used to determine how leaf temperature series predict plant physiological processes like stomatal conductance (Gaur and Drewry 2024). Others have used such methods for predicting photosynthetic performance parameters from plant water status and spectral characteristics (Yang et al. 2022, Song and Wang 2023). A machine learning approach offers

a potential path for ascertaining how leaf temperature profiles might cue changes in heat tolerance thresholds.

Here we measured *in situ* leaf and air temperatures and critical heat tolerance thresholds of photosystem II (PSII) of two co-occurring morphologically and phylogenetically distinct Australian alpine plant species, *Grevillea australis* and *Dracophyllum continentis,* at 16 sites across two locations varying in elevation and landform. By contrasting the aspect and location of study sites, our design maximised the microclimatic variation in terms of the average time of day that maximum temperature occurred, the sum of temperatures across a day and the temperature range of the diurnal cycle. We compared two different approaches to investigate how leaf temperature affects acclimation of plant heat tolerance thresholds. First, representing a traditional statistical approach, we used linear mixed models to determine whether average temperature parameters could explain variations in heat tolerance thresholds. Second, we sought to explain variation in T_{crit} by applying a machine learning (ML) approach, which used the full suite of raw temperature data, representing 5,600 individual leaf temperature points.

Methods

Study site selection and study species

All field and experimental work was conducted on Wolgalu and Monaro Ngarigo lands in Kosciuszko National Park, New South Wales, Australia. Study sites were situated in grasslands at two locations representing different topographies and elevations: Schlink Pass, a sub-alpine, cold air drainage valley along the Munyang River, at 1670 m a.s.l., and Mt Stilwell, an alpine site on the exposed mountain pass above Charlotte Pass Village, 1959 m a.s.l. Aspect, topography and elevation are design features that influence microclimatic conditions. There were 16 sites in total: at each location, eight sites were selected, four of NW aspect and four of SE aspect (Figure 1a; Figure S1; Table S1). Along with the contrasting landforms represented at the two locations, selecting sites with contrasting aspects maximised potential microclimatic variation, based on two factors: first, prevailing winds in the region are from the west to the northwest (AGBoM 2023) and second, incident sunlight is highest for equatorial-facing vegetation (Russell et al. 1989), i.e., north-northwest in the southern hemisphere (for more details, see Supporting Information 1).

The two alpine species, *Dracophyllum continentis* B.L.Burtt (Ericaceae) and *Grevillea australis* R.Br. (Proteaceae), are found in both alpine and subalpine environments throughout South-East Australia. These species were selected because they co-occur in moist alpine environments yet are phylogenetically and morphologically distinct. *Dracophyllum continentis* is a multi-branched shrub growing to 1 m, with thick, ovate to triangular leaves (2–4 cm long, 4–7 mm wide), densely packed around the stem; *G. australis* is a shrub growing to 1 m, with smaller, oblanceolate, linear, or narrow-elliptic leaves (0.5–3.5 cm long, 0.5–5.5 mm wide) that are spread along its woody branches (PlantNET 2024).

Air and leaf temperature measurements

Site-specific air temperature and leaf temperatures of *G. australis* and *D. continentis* were measured at all 16 sites across Schlink Pass and Mt Stilwell from the start of February 2023 (Figure S2a, b). Leaf temperature was logged in 5-minute intervals using fine-wire type-T thermocouples (gauge AWG 36, 0.13 mm diameter, Omega Engineering, Norwalk, CT, USA) connected to four-channel HOBO data loggers (UX120-014M, Onset HOBO® Dataloggers Onset, Bourne, USA). At each site, one thermocouple was attached to the underside of a *D. continentis* leaf and two were attached to *G. australis* leaves. Thermocouples were affixed to the leaves using a small piece of surgical tape, sized to one third of the leaf area to minimise disruption to the leaf boundary layer (Figure S2c, d). All thermocouples measuring leaf temperature were attached to leaves on the outer, sun-exposed north-facing side of the canopy. Another thermocouple measured ambient air temperature and was attached to a branch adjacent to the leaves being measured for temperature. A small white cap covered each air thermocouple to shield it from direct sunlight (Figure S2e, f)**.**

Collection of leaf material

Sampling of leaves for heat tolerance thresholds took place during mid-summer, between 9am and 12pm every day from 26 February to 2 March 2023. To determine the water status of the plants sampled for heat tolerance measurement, we also collected leaves RWC between 25 February and 1 March. The field sites were logistically very challenging to access on foot, so water potential measurements were not feasible. To ensure that heat tolerance measurements were not confounded by time of sampling, leaves were collected from all 16 sites each day by two fieldwork teams concurrently, one at Mt Stilwell and the other at Schlink Pass. At each site, two mature, healthy leaves were collected from the outer sun-

exposed north side of the canopy for each species. Concurrently, a small stem bearing leaves of the same description was collected for relative water content (RWC) measurement. On each day of sampling, leaves were collected from the same plants at each site. After collection, leaves were placed in zip-lock bags lined with damp paper towels and kept in darkness until heat tolerance measurements were made in the laboratory the same day. Leaf samples were measured between five and eight hours after collection (Danzey et al. 2024, Briceño et al. 2025).

Measurement of heat tolerance thresholds

Photosystem II heat tolerance thresholds were measured based on the method detailed by Arnold et al. (2021). Briefly, leaf samples were placed on a thermoelectrically controlled Peltier plate, with type-T thermocouples attached to the underside of each leaf sample for continuous leaf temperature measurements during a controlled heating ramp. The temperature ramp began at 25 °C, increasing at a rate of 0.5 °C per minute until reaching 70 °C. A pulse amplitude modulated imaging fluorimeter (Maxi-Imaging-PAM; Heinz Walz GmbH, Effeltrich, Germany) took measurements of minimal chlorophyll fluorescence (F_0) during heating after allowing 30 minutes for leaves to dark adapt. For each experimental run, 64 T- F_0 curves (two replicates from the 16 sites for each species) were produced, from which the critical heat thresholds (T_{crit}) were determined as the point of transition between slow-rise and fast-rise in F_0 with increasing temperature (Figure S3).

Meausrement of RWC

For relative water content (RWC) determination, leaf samples with petioles removed were first weighed to obtain fresh weight (FW). Samples were then submerged in water-filled pill boxes for 3–4 hours to allow rehydration, after which the turgid weight (TW) was recorded. Subsequently, samples were transported to the laboratory and oven-dried for one week, after which they were re-weighed to obtain the dry weight (DW). RWC was calculated using the formula:

$$\mathrm{RWC} = \frac{\mathrm{FW} - \mathrm{DW}}{\mathrm{TW} - \mathrm{DW}} \times 100$$

Traditional statistical approach for ascertaining the effect of leaf temperature on T_{crit}

To characterise microclimatic variation in thermal profile across study sites, we calculated three temperature parameters that we expected to reflect the nature, intensity and timing of thermal load to which plants are exposed. These factors have been shown to influence plant heat tolerance (Blair et al. 2019, Grinevich et al. 2019, Laosuntisuk and Doherty 2022, Neuner and Buchner 2023, Cook et al. 2024). Heat stress intensity varies with aspect as it determines the timing and magnitude of maximum temperatures in each day (McCune and Keon 2002, Li et al. 2021). Thermal regimes differ markedly between mountain and valley environments. While air temperatures are typically higher in lower elevation environments at night, radiative cooling and cold-air drainage promote the formation of cold air pools, which tend to develop in valleys (Lundquist et al. 2008, Pepin et al. 2022). As such, we chose to calculate the time of day that maximum air temperature was reached (T_{time}^{air}), the daily sum of degrees above 0°C (T_{sum}^{air}), and the diurnal cycle temperature range (T_{range}^{air}) at each of the 16 study sites for the four weeks prior to and coinciding with T_{crit} measurement (Table S2).

First, the temperature data for each site were cleaned to remove non-sensible values due to spurious electrical signals (below -25°C and above 40°C). For calculation of T^{leaf} values for *G. australis*, raw leaf temperature data collected by the two thermocouples were averaged. To calculate T_{sum} values, the average temperatures above 0°C were summed for each five-minute interval across the 24 hours between 12 am and 11:59 pm for each day. For T_{time}, the time at which the maximum temperature occurred on each day was converted into hour values for ease of analysis (e.g., a 24-hour time value of 13:30 became 13.5). T_{range} parameters were calculated by subtracting the minimum temperature occurring each night (between 7 pm and 6:59 am) from the maximum temperature occurring on the subsequent day (between 7 am and 6:59 pm). In addition to calculating 24-hour cumulative temperature above 0 °C (T_{sum}^{leaf}) on T_{crit}, nightly ($T_{sum\text{-}night}^{leaf}$) and daily temperature ($T_{sum\text{-}day}^{leaf}$) sums were calculated separately so we could differentiate between the effects of day and nighttime heat load on T_{crit}. $T_{sum\text{-}day}^{leaf}$ and $T_{sum\text{-}night}^{leaf}$ were calculated by summing the temperatures above 0°C for each 5-minute interval between 7 am and 6:59 pm and 7 pm and 6:59 am respectively. Individual daily values for each T^{air} parameter at each site were averaged across all days of February, resulting in 16 levels of each microclimate parameter. Values for each T^{leaf} parameter were averaged at each site and for each species across the

days preceding and coinciding with T_{crit} sampling (22 Feb – 28 Feb) resulting in 32 levels of each leaf temperature parameter.

To assess whether plants from these distinct microclimates differed in water status, we fitted an LMM with the same structure as above, but with RWC as the response variable and plant ID included as an additional random factor and species as an additional fixed factor. While RWC differed significantly between species ($F_{1, 27} = 52.9$, $p < 0.001$), it did not with location ($F_{1, 27} = 0.43$, $p = 0.52$) or aspect ($F_{1, 27} = 0.0059$, $p = 0.0.94$; Figure S4). This analysis enabled us to exclude variation in plant water status across sites as a factor potentially confounding microclimatic variation in T_{crit}.

Having established that T_{time}^{air}, T_{sum}^{air} and T_{range}^{air} reflect the substantial microclimatic variation among sites (Table S3), we next sought to determine the influence of the equivalent leaf temperature versions of these parameters on heat tolerance thresholds. Leaf temperature parameters (T_{time}^{leaf}, T_{sum}^{leaf} and T_{range}^{leaf}) were calculated using the measured leaf temperatures of *G. australis* and *D. continentis* spanning the four days prior to, and first three days of T_{crit} sampling (Figure S5), which we expected to most closely reflect the temperature conditions likely to initiate changes in heat tolerance thresholds (Bison and Michaletz 2024, Zhu et al. 2024). In addition to calculating 24-hour cumulative temperature above 0 °C (T_{sum}^{leaf}) on T_{crit}, nightly ($T_{sum\text{- }night}^{leaf}$) and daily temperature ($T_{sum\text{- }day}^{leaf}$) sums were calculated separately so we could differentiate between the effects of day and nighttime heat load on $T_{crit.}$. All temperature parameters were averaged across the seven days for each of the 16 sites and the resulting values were included as fixed factors in three separately fitted LMMs, where T_{crit} was the response variable. In each model, date was included as a random factor to account for weather variation across sampling days. To prevent boundary fit issues arising from including aspect and location separately, a categorical variable named 'site type' with four levels (SchlinkSE, SchlinkNW, StilwellNW, StilwellSE) was used as a random factor in these models. Where boundary fit issues persisted, 'site type' was removed from the model. An additional random effect was added to the models, Plant ID, of which there were 32 levels, to account for variability between leaf replicates. 'Species' was excluded from $T^{leaf} \sim T_{crit}$ models as a fixed term because preliminary analyses determined that T_{crit} did not differ between species ($F_{1, 286} = 0.087$, $p =$

0.77). Analyses were conducted using R Statistical Software (v 4.2.1: R Development Core Team 2024).

Machine learning approach to ascertaining the effect of leaf temperature on T_{crit}

Boosting-based ensemble methods are a class of machine learning algorithms that combine multiple decision trees into a single strong predictive model. Each decision tree is trained sequentially, with each subsequent model attempting to correct the residual errors of its predecessor. This learning process allows boosting models to capture complex, nonlinear relationships between input, predictive features and response variables (Natekin and Knoll 2013). We utilised the IBM Watson Machine Learning platform to train a Snap Boosting Machine Regressor model to identify key predictive temperature points leading up to T_{crit} measurements. For the machine learning model (Python script) see Supplementary File 1. Five-minute interval leaf temperature data from both species and all sites were pooled together for training the model. This pooled model resulted in 153 T_{crit} values with their respective temperature history, which initially encompassed 25 days prior to each T_{crit} measurement (1 February 2023 – 1 March 2023; 8,532 time points and 267,264 leaf temperature points for each day of T_{crit} measurement for the initial 29-day model). Based on this preliminary analysis, we narrowed this down to the four-day temperature history leading up to each T_{crit} measurement (1,152 time points and 36,864 leaf temperatures points for each day of T_{crit} measurement, Figure S6), as it provided the most relevant predictive features. This decision was supported by literature on the biochemical processes that govern heat tolerance; for example, decay of upregulated heat shock proteins has been shown to occur between 2 and 3 days after heat stress (Charng et al. 2006, Aspinwall et al. 2019). These findings align with the three days prior to T_{crit} measurement being the best predictive window for shifts in heat tolerance (Bison and Michaletz 2024, Zhu et al. 2024).

Results

T^{leaf} parameters appear to predict little variation in T_{crit}

Three leaf temperature parameters (T_{time}^{leaf}, T_{sum}^{leaf} and T_{range}^{leaf}) were included as fixed factors in separate LMMs where T_{crit} was the response variable (Table 2). Accounting for site type (location-aspect combination: SchlinkNW, SchlinkSE, StilwellNW, StilwellSE), T_{sum}^{leaf} predicted significant variation in T_{crit}, such that for a 313.5°C increase in T_{sum}^{leaf}, T_{crit} increased

by 1°C (Table 2, Figure 2b). No significant relationship of T_{time}^{leaf}, $T_{sum\text{-}day}^{leaf}$, $T_{sum\text{-}night}^{leaf}$ T_{range}^{leaf} with T_{crit} was found (Table 2, Figure 2c, d; Figure S7; Table S4). The reason that the positive $T_{sum}^{leaf} \sim T_{crit}$ relationship was relatively weak might be attributed to the nature of the variation in T_{crit} across sampling days. Although date was a strong predictor of variation in T_{crit}, the only day where T_{crit} was significantly different from the rest was on 28 Feb. T_{crit} values were on average 2.8 ± 0.9°C higher on 28 Feb than the rest but across all other days, T_{crit} values were relatively uniform (Figure 2a). To assess whether these elevated 28 February values were driving the significant $T_{sum}^{leaf} \sim T_{crit}$ relationship, we re-ran the model with these values excluded. The relationship was no longer significant, indicating that the 28 February T_{crit} values were indeed responsible for the original significance.

Machine learning reveals that preceding high and low temperatures can predict T_{crit}

The machine learning results highlighted specific temperatures and times within the temperature histories that were critical for predicting T_{crit} (coloured circles, Figure 3a). A total of 33 leaf temperature time points within the four-day temperature window, which were common to all leaves, were identified as collectively contributing 84.9% of the model's total predictive power. The identified times points were predominantly high and low leaf temperature values within the four-day period preceding T_{crit} measurement. The strength of predictive power was distributed relatively uniformly across the 4-day period. Three leaf temperature points, however, one maximum and two minima occurring between 81 and 45 h prior to T_{crit} measurement, provided 36.8% of the total predictive power (grey ellipses, Figure 3b).

Discussion

The current study sought to determine how spatially and temporally varying leaf temperatures drive changes in T_{crit} photosystem heat thresholds using two distinct approaches: linear mixed models (LMMs) and machine learning (ML). Specifically, we were interested in the insights that each method could provide about the role of prior leaf temperature history in determining these thresholds, a question that has been explored little to date. Temperature regimes show considerable spatial variation in alpine environments, especially as a function of elevation and aspect (Legates and Willmott 1990, McCune and Keon 2002). In our study, microclimatic variation with aspect and elevation was

characterised by different times of day that maximum air temperatures were reached, the sum or load of temperature and the diurnal cycle temperature range. However, LMMs revealed that the only corresponding leaf temperature parameter that predicted variation in photosystem heat thresholds was average daily heat sum (T_{sum}^{leaf}) and that relationship was weak. Whereas leaf temperature parameters were not compelling predictors of T_{crit} based on LMMs, the novel ML approach was able to account for the complexity of the entire thermal profile. Machine learning revealed that leaf temperature extremes, both high and low, within the four days preceding heat tolerance measurements explained nearly 85% of the variation in T_{crit}.

Increases in mean daily heat load weakly correlates with increases in T_{crit}

Mounting evidence suggests that photosystem heat tolerance thresholds respond to local thermal conditions, varying temporally (Neuner et al. 2000, Coast et al. 2022, Posch et al. 2022) and spatially (Curtis et al. 2016, O'Sullivan et al. 2017, Cook et al. 2021, Danzey et al. 2024, Kullberg and Feeley 2024)**.** While averages of point leaf temperature measurements are typically used to characterise the conditions to which a plant is exposed, these metrics do not capture the complex range of thermal conditions, nor the cumulative nature of heat stress, which have important implications on measuring shifts in physiological tolerance (Neuner and Buchner 2023, Cook et al. 2024, Faber et al. 2024). The weak $T_{sum}^{leaf} \sim T_{crit}$ relationship was driven by high T_{crit} values on 28 Feb. This relationship may have been weakened due to the relatively benign leaf temperatures in the week leading up to T_{crit} measurement (22.5°C on average). Interestingly, no significant relationship of $T_{sum\text{-}day}^{leaf}$ or $T_{sum\text{-}night}^{leaf}$ with T_{crit} was observed. This finding suggests that thermal tolerance cannot be understood by examining daytime or nighttime conditions in isolation. Given that sites clearly had different microclimatic profiles through time, these findings suggest that LMM analytical approaches that average across substantial daily leaf temperature variation obscure biologically important information.

Machine learning reveals preceding temperature extremes that predict shifts in T_{crit}

Using machine learning, we found compelling evidence that certain daily leaf temperature points prior to measurement predict subsequent shifts in T_{crit}. The extremes of daily maximum and, importantly, nightly minimum temperatures up to four days prior to heat threshold measurement predicted a combined 85% of the variation in T_{crit}. The field of

cross-tolerance, where exposure to one kind of stress results in tolerance to another (Hossain et al. 2018), may explain this potentially counterintuitive pattern. Harris et al. (2024) found that the occurrence of a hot day in concert with a cold night increases heat tolerance more than a hot day and warm night, suggesting that exposure to cold stress improves tolerance to heat stress. Indeed, both types of thermal stress can activate similar response pathways (Mei and Song 2010, Li et al. 2014, Hossain et al. 2018). Heat shock proteins (HSPs) are known to upregulate in response to both heat and cold stress (Anderson et al. 1994, Wang et al. 2003), with small HSPs (common in plant chloroplasts) detectable for up to 72 h after a triggering event (Charng et al. 2006). Further, there is evidence to suggest that increases in reactive oxygen species and subsequent upregulation of antioxidant enzymes are involved in the deployment of cross-tolerance (Gong et al. 2001, Hossain et al. 2016, Hossain et al. 2018).

In the current study, lower nightly temperatures followed by higher daily temperatures might have had an acclimatory effect on heat tolerance by activating similar response pathways, which manifested as increased T_{crit} in the days following. Danzey et al. (2024) foundPSII cold tolerance thresholds of -10.8 °C for *G. australis* and -10.3 °C for *D. continentis*. In our study, the average of nightly leaf temperatures across the 7-day window preceding T_{crit} measurements were –2.8 °C and –3.3 °C for *G. australis* and *D. continentis,* respectively, with leaf temperatures dropping as low as -6.9 °C across this period. While these temperatures did not surpass the reported cold tolerance thresholds, they approached this range. Repeated exposure to near cold thresholds likely contributed to the observed acclimation. Conversely, maximum temperatures approached heat tolerance thresholds measured in the current study much less closely; average maximum leaf temperature across sites and both species was 22.5 ± 0.26 °C, while average T_{crit} was 47.8 ± 0.2 °C. Such disparities between maximum temperatures and temperature thresholds have been observed by others, particularly in cooler climate species (Buchner and Neuner 2003, Kitudom et al. 2022, Cox et al. 2025). The stress induced by consistent low-grade stress can equate to that incurred by short, intense temperature stress (Neuner and Buchner 2023, Cook et al. 2024, Arnold et al. 2025b). In the context of the present study, it is plausible that the moderate maximum leaf temperatures observed maintained relatively high baseline T_{crit} values. Further, plants from environments with high seasonal or interannual variability may

maintain elevated T_{crit} as a buffer against rare but damaging extremes. Although our 5-min averages showed mid-20 °C maxima, brief spikes (e.g., 30–35 °C) may have been missed yet sufficient to induce acclimation, especially because induction temperatures can lie well below damage thresholds (Knight and Ackerly 2002). As well as prior exposure to heat stress, increased heat tolerance in plants can be induced by priming with other abiotic stressors, such as drought exposure can also enhance heat tolerance (Ru et al. 2022, Sumner et al. 2022, Yadav et al. 2022, Kamran et al. 2025). In this study, drought stress was unlikely to be a confounding factor because relative water content remained consistent across site types (Figure S4) and rarely declined to levels indicative of water stress during the sampling period. An alternative explanation for why both maximum and minimum leaf temperature predict heat threshold shifts is rapid acclimation and subsequent de-acclimation, which frequently occur in thermally fluctuating alpine environments (Buchner and Neuner 2003). Rapid acclimatory responses maybe associated with diurnal alterations of sugar concentrations and osmotic potential (Seemann et al. 1986, Meyer and Santarius 1998, Coast et al. 2022). Average daily maximum temperatures in alpine environments may not seem stressful in absolute terms, but a sufficiently large diurnal swing between minima and maxima could be. In our study, leaf temperature maxima in the days prior to T_{crit} measurements might have primed leaves for subsequent high temperatures, such that a cold night followed by another hot day would lead to an acclimatory shift in T_{crit}. Plants may have de-acclimated when exposed to lower day time temperatures on 26 February (Figure S5). When temperatures rose on 27–28 February, plants likely re-acclimated, reflected in the higher T_{crit} measured on 28 February. This sequence of de-acclimation and subsequent re-acclimation over 27–28 February likely drove the significant $T_{sum} \sim T_{crit}$ relationship. Acclimation of T_{crit} within a three-day window has recently been observed by others (Bison and Michaletz 2024), perhaps underpinned by upregulation of HSPs and changes in membrane fatty acid composition (Zhu et al. 2024) and/or by expression of genes or isoforms associated with photosynthesis and solute transport (Roces et al. 2022). Because the ability of machine learning to identify lag effects of temperature fluctuations on T_{crit} is not predicated on linear relationships, the approach is well-suited for capturing these complex acclimation dynamics, especially in field conditions, where environmental conditions fluctuate frequently.

Irrespective of how these extreme temperatures triggered shifts in heat tolerance, the same response was evident for both species. No differences in the predictive points were seen between species when separate machine-learning analyses were performed for them (results not shown). Likewise, when testing for the main effects of species using linear mixed models, no significant effect of species on T_{crit} was found. Growth form and leaf traits, including but not limited to, leaf angle, leaf mass per area and leaf habit have been reported as being significant predictors of heat tolerance (Sklenář et al. 2016, Sastry and Barua 2017, Leon-Garcia and Lasso 2019, Middleby et al. 2025). Further, transpiration rates influence leaf energy balance and perhaps heat tolerance thresholds (Marchin et al. 2022, Valliere et al. 2023). It is, therefore, possible that because *G. australis* and *D. continentis* are both evergreen alpine shrubs of similar heights, differences in leaf temperature driven by leaf structural traits or transpiration (Bird et al. unpublished data) might not have been great enough to cause differences in T_{crit}. We note, however, our restriction to just two species limits the ability to draw general conclusions about different species responses, something that warrants further research.

Conclusions and future directions

Our findings indicate that not only temporally proximal leaf temperature maxima, but also minima play a significant role in triggering shifts in heat tolerance thresholds. Our study also corroborated the importance of cumulative heat load in determining heat tolerance thresholds. However, this direct cumulative effect was small, highlighting that average leaf temperature parameters do not sufficiently capture the temporal variability in thermal conditions that influence physiological tolerance thresholds. By contrast, machine learning revealed patterns that traditional statistical methods could not, providing new insights into acclimatory triggers for shifts in thermal tolerance threshold. The observation that both high and low temperature extremes are important predictors of T_{crit} underscores the importance of considering both ends of the temperature spectrum when predicting plant responses to heat stress. Future studies should investigate whether cross tolerance represents a competitive advantage for species from thermally variable environments. With a larger sample size and broader range of species, machine learning may reveal the requirements for thermal cues to induce cross-tolerance responses. Additionally, such an approach may clarify

whether acclimation to temperatures in the four days preceding threshold measurement is a consistent and generalisable phenomenon.

In summary, while statistical approaches are useful for understanding broad ecological patterns, machine learning could be particularly useful when dealing with spatially and temporally fluctuating environmental conditions and where their relationships with plant physiology are complex and non-linear. Combining machine learning with more traditional statistical approaches could enhance predictive accuracy, enabling the development of robust tools to guide ecosystem management, conservation strategies, and climate resilience efforts.

Author contributions

CP, AL, PA, SG, AN, AH and LD conceived of and designed the project; CP, MB and LD conducted site selection and field work; CP conducted physiological measurements; CP, LD, PA and AH carried out data analyses; CP and AL lead the writing; all authors contributed to writing.

Acknowledgements

This work was conducted on the traditional lands and waters of the Ngarigo, Walgalu, Ngunnawal, Ngambri and Gadigal; we acknowledge their Elders, past, present and emerging. We are grateful for the help of field volunteers: Lisa Danzey, Jeanette Jeffreys, Finn Billyard-Currey, Jay Nicholson, Michelle Bird and Anne Pottinger. The research was conducted in association with Australian Research Council Linkage Project grant: LP180100942.

References

AGBoM (2023) Rose of Wind direction versus Wind speed in km/h: Charlotte Pass (Kosciusko Chalet).

Alvarez PR, Harris RJ, Cook AM, Briceño VF, Nicotra AB, Leigh A (2025) Native Australian seedlings exhibit novel strategies to acclimate to repeated heatwave events. Oecologia 207(6): 84

Anderson JV, Li QB, Haskell DW, Guy CL (1994) Structural organization of the spinach endoplasmic reticulum-luminal 70-kilodalton heat-shock cognate gene and expression of 70-kilodalton heat-shock genes during cold acclimation. Plant Physiology 104(4): 1359–1370

Andrew SC, Arnold PA, Simonsen AK, Briceño VF (2023) Consistently high heat tolerance acclimation in response to a simulated heatwave across species from the broadly distributed Acacia genus. Functional Plant Biology 50(1): 71–83

Arnold PA, Briceño VF, Gowland KM, Catling AA, Bravo LA, Nicotra AB (2021) A high-throughput method for measuring critical thermal limits of leaves by chlorophyll imaging fluorescence. Functional Plant Biology 48(6): 634–646

Arnold PA, White MJ, Cook AM, Leigh A, Briceño VF, Nicotra AB (2025a) Plants originating from more extreme biomes have improved leaf thermoregulation. Annals of Botany 136(1): 199–213

Arnold PA, Noble DWA, Nicotra AB, Kearney MR, Rezende EL, Andrew SC, Briceño VF, Buckley LB, Christian KA, Clusella-Trullas S, Geange SR, Guja LK, Jiménez Robles O, Kefford BJ, Kellermann V, Leigh A, Marchin RM, Mokany K, Bennett JM (2025b) A Framework for Modelling Thermal Load Sensitivity Across Life. Global Change Biology 31(7): e70315

Aspinwall MJ, Pfautsch S, Tjoelker MG, Vårhammar A, Possell M, Drake JE, Reich PB, Tissue DT, Atkin OK, Rymer PD, Dennison S, Van Sluyter SC (2019) Range size and growth temperature influence Eucalyptus species responses to an experimental heatwave. Global Change Biology 25(5): 1665–1684

494 Bird M, Pottinger C, Arnold P, Danzey L, Geange S, Kearney M, Nicotra A, Leigh A
495 (unpublished data) Can NicheMapR predict leaf temperatures of morphologically
496 disparate species across microclimatically distinct alpine sites?

497 Bison NN, Michaletz ST (2024) Variation in leaf carbon economics, energy balance, and heat
498 tolerance traits highlights differing timescales of adaptation and acclimation. New
499 Phytologist 242(5): 1919–1931

500 Blair EJ, Bonnot T, Hummel M, Hay E, Marzolino JM, Quijada IA, Nagel DH (2019)
501 Contribution of time of day and the circadian clock to the heat stress responsive
502 transcriptome in Arabidopsis. Scientific Reports 9(1): 4814

503 Blonder B, Michaletz ST (2018) A model for leaf temperature decoupling from air
504 temperature. Agricultural and Forest Meteorology 262: 354–360

505 Briceño VF, Arnold PA, Cook AM, Courtney Jones SK, Gallagher RV, French K, Bravo LA,
506 Nicotra AB, Leigh A (2025) Drivers of thermal tolerance breadth of plants across
507 contrasting biomes. Journal of Ecology in press

508 Buchner O, Neuner G (2003) Variability of heat tolerance in alpine plant species measured at
509 different altitudes. Arctic, Antarctic, and Alpine Research 35(4): 411–420, Article

510 Charng YY, Liu HC, Liu NY, Hsu FC, Ko SS (2006) Arabidopsis Hsa32, a novel heat shock
511 protein, is essential for acquired thermotolerance during long recovery after
512 acclimation. Plant Physiology 140(4): 1297–1305

513 Coast O, Posch BC, Rognoni BG, Bramley H, Gaju O, Mackenzie J, Pickles C, Kelly AM, Lu M,
514 Ruan Y-L, Trethowan R, Atkin OK (2022) Wheat photosystem II heat tolerance:
515 evidence for genotype-by-environment interactions. The Plant Journal 111(5): 1368–
516 1382

517 Cook AM, Berry N, Milner KV, Leigh A (2021) Water availability influences thermal safety
518 margins for leaves. Functional Ecology 35(10): 2179–2189, Article

519 Cook AM, Rezende EL, Petrou K, Leigh A (2024) Beyond a single temperature threshold:
520 Applying a cumulative thermal stress framework to plant heat tolerance. Ecology
521 Letters 27(3): e14416

522 Cox D, Marchin RM, Ellsworth DS, Wujeska-Klause A, Ossola A, Crous KY, Leishman MR,
523 Rymer PD, Tjoelker MG (2025) Thermal Safety Margins and Peak Leaf Temperatures
524 Predict Vulnerability of Diverse Plant Species to an Experimental Heatwave. Plant,
525 Cell & Environment in press

526 Curtis E (2017) Spatiotemporal dynamics of high-temperature tolerance in australian arid-
527 zone plants. University of Technology, Sydney,

528 Curtis EM, Gollan J, Murray BR, Leigh A (2016) Native microhabitats better predict tolerance
529 to warming than latitudinal macro-climatic variables in arid-zone plants. Journal of
530 Biogeography 43(6): 1156–1165

531 Danzey LM, Briceño VF, Cook AM, Nicotra AB, Peyre G, Rossetto M, Yap JS, Leigh A (2024)
532 Environmental and Biogeographic Drivers behind Alpine Plant Thermal Tolerance
533 and Genetic Variation. Plants (Basel) 13(9)

534 Donat MG, Alexander LV (2012) The shifting probability distribution of global daytime and
535 night-time temperatures. Geophysical Research Letters 39(14): e14707

536 Easterling DR, Horton B, Jones PD, Peterson TC, Karl TR, Parker DE, Salinger MJ, Razuvayev
537 V, Plummer N, Jamason P, Folland CK (1997) Maximum and Minimum Temperature
538 Trends for the Globe. Science 277(5324): 364–367

539 Faber A, Ørsted M, Ehlers K (2024) Application of the thermal death time model in
540 predicting thermal damage accumulation in plants. Journal of Experimental Botany
541 75(11): 3467–3482

542 Fauset S, Freitas HC, Galbraith DR, Sullivan MJP, Aidar MPM, Joly CA, Phillips OL, Vieira SA,
543 Gloor MU (2018) Differences in leaf thermoregulation and water use strategies
544 between three co-occurring Atlantic forest tree species. Plant, Cell & Environment
545 41(7): 1618–1631

546 Feeley K, Martinez-Villa J, Perez T, Silva Duque A, Triviño Gonzalez D, Duque A (2020) The
547 Thermal Tolerances, Distributions, and Performances of Tropical Montane Tree
548 Species. Frontiers in Forests and Global Change 3, Original Research

549 Gaur S, Drewry DT (2024) Explainable machine learning for predicting stomatal conductance
550 across multiple plant functional types. Agricultural and Forest Meteorology 350:
551 e109955

552 Gong M, Chen Bo, Li Z-G, Guo L-H (2001) Heat-shock-induced cross adaptation to heat,
553 chilling, drought and salt stress in maize seedlings and involvement of H2O2. Journal
554 of Plant Physiology 158(9): 1125–1130

555 Grinevich D, Stroup K, Duan J, Slabaugh E, Doherty C (2019) Novel transcriptional responses
556 to heat revealed by turning up the heat at night. Plant Molecular Biology 101(1): 1–
557 19

558 Harris RJ, Alvarez PR, Bryant C, Briceño VF, Cook AM, Leigh A, Nicotra AB (2024) Acclimation
559 of thermal tolerance in juvenile plants from three biomes is suppressed when
560 extremes co-occur. Conservation Physiology 12(1): coae027

561 Hossain MA, Burritt DJ, Fujita M (2016) Cross-Stress Tolerance in Plants: Molecular
562 Mechanisms and Possible Involvement of Reactive Oxygen Species and
563 Methylglyoxal Detoxification Systems. pp 327–380

564 Hossain MA, Li Z-G, Hoque TS, Burritt DJ, Fujita M, Munné-Bosch S (2018) Heat or cold
565 priming-induced cross-tolerance to abiotic stresses in plants: key regulators and
566 possible mechanisms. Protoplasma 255(1): 399–412

567 Hüve K, Bichele I, Tobias M, Niinemets U (2006) Heat sensitivity of photosynthetic electron
568 transport varies during the day due to changes in sugars and osmotic potential. Plant
569 Cell & Environment 29(2): 212–228

570 Kamran M, Burdiak P, Karpiński S (2025) Crosstalk Between Abiotic and Biotic Stresses
571 Responses and the Role of Chloroplast Retrograde Signaling in the Cross-Tolerance
572 Phenomena in Plants. Cells 14(3): 176

573 Kitudom N, Fauset S, Zhou Y, Fan Z, Li M, He M, Zhang S, Xu K, Lin H (2022) Thermal safety
574 margins of plant leaves across biomes under a heatwave. Science of The Total
575 Environment 806: 150416

576 Knight C, Ackerly D (2002) An ecological and evolutionary analysis of photosynthetic
577 thermotolerance using the temperature-dependent increase in fluorescence.
578 Oecologia 130(4): 505–514

579 Knight CA, Ackerly DD (2003) Evolution and plasticity of photosynthetic thermal tolerance,
580 specific leaf area and leaf size: congeneric species from desert and coastal
581 environments. New Phytologist 160(2): 337–347

582 Körner C (2003) Alpine Plant Life: Functional Plant Ecology Of High Mountain Ecosystems.
583 Springer, Germany

584 Körner C (2023) Concepts in Alpine Plant Ecology. Plants 12(14): 2666

585 Körner C, Cochrane P (1983) Influence of plant physiognomy on leaf temperature on clear
586 midsummer days in the Snowy Mountains, south-eastern Australia. Acta Oecologia
587 4: 117–124

588 Körner C, Hiltbrunner E (2021) Why is the alpine flora comparatively robust against climatic
589 warming? Diversity 13(8): 383

590 Kullberg AT, Feeley KJ (2024) Seasonal acclimation of photosynthetic thermal tolerances
591 in six woody tropical species along a thermal gradient. Functional Ecology 38(11):
592 2493–2505

593 Laosuntisuk K, Doherty CJ (2022) The intersection between circadian and heat-responsive
594 regulatory networks controls plant responses to increasing temperatures. Biochem
595 Soc Trans 50(3): 1151–1165

596 Legates DR, Willmott CJ (1990) Mean seasonal and spatial variability in global surface air
597 temperature. vol 41.

598 Leigh A, Sevanto S, Close JD, Nicotra AB (2017) The influence of leaf size and shape on leaf
599 thermal dynamics: does theory hold up under natural conditions? Plant, Cell &
600 Environment 40(2): 237–248

601 Leon-Garcia IV, Lasso E (2019) High heat tolerance in plants from the Andean highlands:
602 Implications for paramos in a warmer world. PLoS One 14(11): e0224218

603 Li S-L, Xia Y-Z, Liu J, Shi X-D, Sun Z-Q (2014) Effects of cold-shock on tomato seedlings under
604 high temperature stress. The Journal of Applied Ecology 25: 2927–2934

605 Li Xe, Song X, Zhao J, Lu H, Qian C, Zhao X (2021) Shifts and plasticity of plant leaf mass per
606 area and leaf size among slope aspects in a subalpine meadow. Ecology and
607 Evolution 11(20): 14042–14055

608 Lundquist JD, Pepin N, Rochford C (2008) Automated algorithm for mapping regions of cold-
609 air pooling in complex terrain. Journal of Geophysical Research: Atmospheres
610 113(D22)

611 Marchin RM, Backes D, Ossola A, Leishman MR, Tjoelker MG, Ellsworth DS (2022) Extreme
612 heat increases stomatal conductance and drought-induced mortality risk in
613 vulnerable plant species. Global Change Biology 28(3): 1133–1146

614 McCune B, Keon D (2002) Equations for potential annual direct incident radiation and heat
615 load. Journal of vegetation science 13(4): 603–606

Mei YQ, Song SQ (2010) Response to temperature stress of reactive oxygen species scavenging enzymes in the cross-tolerance of barley seed germination. Journal of Zhejiang University Science B 11(12): 965–972

Meyer H, Santarius KA (1998) Short-term thermal acclimation and heat tolerance of gametophytes of mosses. Oecologia 115(1-2): 1–8

Middleby KB, Cheesman AW, Hopkinson R, Baker L, Ramirez Garavito S, Breed MF, Cernusak LA (2025) Ecotypic Variation in Leaf Thermoregulation and Heat Tolerance but Not Thermal Safety Margins in Tropical Trees. Plant, Cell & Environment 48(1): 649–663

Natekin A, Knoll A (2013) Gradient boosting machines, a tutorial. Front Neurorobot 7: 21

Neuner G, Buchner O (2012) Dynamics of Tissue Heat Tolerance and Thermotolerance of PS II in Alpine Plants. In: Lütz C (ed) Plants in Alpine Regions: Cell Physiology of Adaption and Survival Strategies. Springer Vienna, Vienna, pp 61–74

Neuner G, Buchner O (2023) The dose makes the poison: The longer the heat lasts, the lower the temperature for functional impairment and damage. Environmental and Experimental Botany 212(4): 105395

Neuner G, Buchner O, Braun V (2000) Short-term changes in heat tolerance in the alpine cushion plant silene acaulis ssp. Excapa [all.] j. Braun at different altitudes. Plant Biology 2(6): 677–683

Niu Y, Xiang Y (2018) An Overview of Biomembrane Functions in Plant Responses to High-Temperature Stress. Frontiers in Plant Science 9: 915

O'Sullivan O, Heskel M, Reich P, Tjoelker M, Weerasinghe L, Penillard A, Zhu L, Egerton J, Bloomfield K, Creek D, Bahar N, Griffin K, Hurry V, Meir P, Turnbull M, Atkin O (2017) Thermal limits of leaf metabolism across biomes. Global Change Biology 23(1): 209–223

Pepin NC, Arnone E, Gobiet A, Haslinger K, Kotlarski S, Notarnicola C, Palazzi E, Seibert P, Serafin S, Schöner W, Terzago S, Thornton JM, Vuille M, Adler C (2022) Climate changes and their elevational patterns in the mountains of the world. Reviews of Geophysics 60(1)

Perez TM, Feeley KJ (2020) Photosynthetic heat tolerances and extreme leaf temperatures. Functional Ecology 34(11): 2236–2245

PlantNET (2024) (The NSW Plant Information Network System). Royal Botanic Gardens and Domain Trust, Sydney

Posch BC, Hammer J, Atkin OK, Bramley H, Ruan Y-L, Trethowan R, Coast O (2022) Wheat photosystem II heat tolerance responds dynamically to short- and long-term warming. Journal of Experimental Botany 73(10): 3268–3282

R Development Core Team (2024) R: A language and environment for statistical computing. R Foundation for Statistical Computing, Vienna, Austria

Rahnama A, Salehi F, Meskarbashee M, Mehdi Khanlou K, Ghorbanpour M, Harrison MT (2024) High temperature perturbs physicochemical parameters and fatty acids composition of safflower (Carthamus tinctorius L.). BMC Plant Biology 24(1): 1080

Roces V, Lamelas L, Valledor L, Carbó M, Cañal MJ, Meijón M (2022) Integrative analysis in Pinus revealed long-term heat stress splicing memory. The Plant Journal 112(4): 998–1013

Ru C, Hu X, Chen D, Wang W, Song T (2022) Heat and drought priming induce tolerance to subsequent heat and drought stress by regulating leaf photosynthesis, root morphology, and antioxidant defense in maize seedlings. Environmental and Experimental Botany 202: 105010

Russell G, Marshall B, Jarvis PG (1989) Plant canopies: their growth, form and function. Cambridge University Press, Cambridge & New York

Sastry A, Barua D (2017) Leaf thermotolerance in tropical trees from a seasonally dry climate varies along the slow-fast resource acquisition spectrum. Scientific Reports 7(1): 11246

Seemann JR, Downton WJ, Berry JA (1986) Temperature and leaf osmotic potential as factors in the acclimation of photosynthesis to high temperature in desert plants. Plant Physiology 80(4): 926–930

Sklenář P, Kučerová A, Macková J, Romoleroux K (2016) Temperature microclimates of plants in a tropical alpine environment: how much does growth form matter? Arctic, Antarctic, and Alpine Research 48(1): 61–78

Song G, Wang Q (2023) Coupling effective variable selection with machine learning techniques for better estimating leaf photosynthetic capacity in a tree species (Fagus crenata Blume) from hyperspectral reflectance. Agricultural and Forest Meteorology 338: 109528

Sumner EE, Williamson VG, Gleadow RM, Wevill T, Venn SE (2022) Acclimation to water stress improves tolerance to heat and freezing in a common alpine grass. Oecologia 199(4): 831–843

Valliere JM, Nelson KC, Martinez MC (2023) Functional traits and drought strategy predict leaf thermal tolerance. Conservation Physiology 11(1): coad085

Vilas-Boas T, Almeida HAd, Della Torre F, Modolo LV, Lovato MB, Lemos-Filho JP (2024) Intraspecific variation in the thermal safety margin in Coffea arabica L. in response to leaf age, temperature, and water status. Scientia Horticulturae 337: 113455

Wahid A, Gelani S, Ashraf M, Foolad MR (2007) Heat tolerance in plants: An overview. Environmental and Experimental Botany 61(3): 199–223

Wang W, Vinocur B, Altman A (2003) Plant responses to drought, salinity and extreme temperatures: towards genetic engineering for stress tolerance. Planta 218(1): 1–14

Willits DH, Peet MM (1998) The effect of night temperature on greenhouse grown tomato yields in warm climates. Agricultural and Forest Meteorology 92(3): 191–202

Yadav R, Juneja S, Kumar R, Saini R, Kumar S (2022) Understanding cross-tolerance mechanism and effect of drought priming on individual heat stress and combinatorial heat and drought stress in chickpea. Journal of Crop Science and Biotechnology 25(5): 515–533

Yang Z, Tian J, Wang Z, Feng K (2022) Monitoring the photosynthetic performance of grape leaves using a hyperspectral-based machine learning model. European Journal of Agronomy 140: 126589

Zhang X, Rademacher T, Liu H, Wang L, Manzanedo RD (2023) Fading regulation of diurnal temperature ranges on drought-induced growth loss for drought-tolerant tree species. Nature Communications 14(1): 6916

Zhu L, Scafaro A, Vierling E, Ball M, Posch B, Stock F, Atkin O (2024) Heat tolerance of a tropical–subtropical rainforest tree species Polyscias elegans: time-dependent dynamic responses of physiological thermostability and biochemistry. New Phytologist 241(2): 715–731

Zhu L, Bloomfield KJ, Hocart CH, Egerton JJ, O'Sullivan OS, Penillard A, Weerasinghe LK, Atkin OK (2018) Plasticity of photosynthetic heat tolerance in plants adapted to thermally contrasting biomes. Plant, Cell & Environment 41(6): 1251–1262

Figure legends

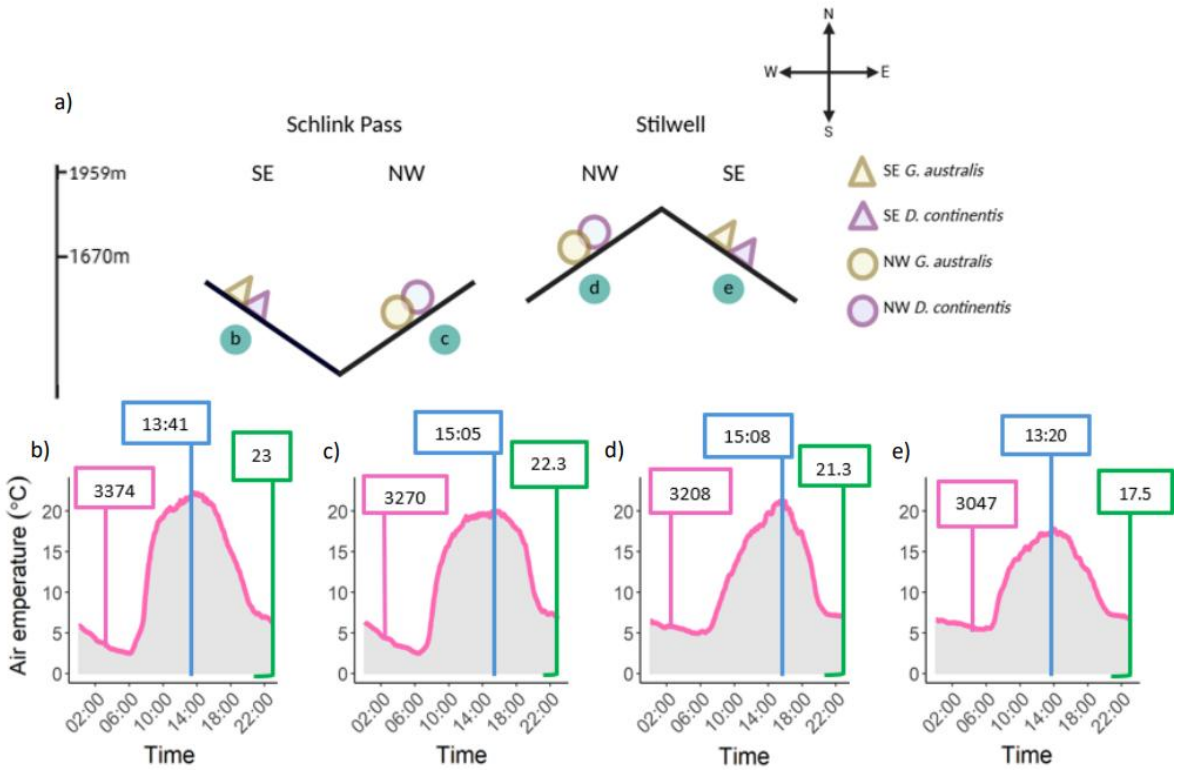

Figure 1. A schematic of the experimental design capturing microclimatic variation. a) site and aspect contrasts; both species (*Grevillea australis* and *Dracophyllum continentis*) at study sites contrasting in aspect throughout Schlink Pass and Mt Stilwell. The average elevation of sites at each location can be seen on the left. Black letters in green circles correspond with a site type, the air temperature parameters of which are indicated in panels b, c, d and e. T_{sum}^{air} (°C) represents the daily average sum of degrees above 0°C occurring at 5-minute intervals across a 24-hr period (pink boxes, left); T_{time}^{air} represents the time of day at which maximum air temperatures occurred (blue boxes, middle) and T_{range}^{air} (°C) represents the diurnal range of air temperature (green boxes, right). Daily values for all three parameters were averaged across the month of February 2023 and across the four replicates of each site type (SchlinkSE, SchlinkNW, StilwellNW and StilwellSE). For full details, see Tables S1 and S2.

Table 1. The output of linear mixed models to determine the influence of aspect (NW v SE) and location (Schlink Pass v Mt Stilwell) on site-specific daily heat sum (T_{sum}^{air}), time of day that maximum temperatures were reached (T_{time}^{air}) and diurnal temperature range (T_{range}^{air}) across the month of February 2023.The model included the sampling date as a random factor to account for variation in heat sum caused by differences in weather across days (Figure S5). Bolded p-values indicate significance at $\alpha = 0.05$.

Response variable	**df**	**Fixed effects**	**F**	**p-value**
T_{time}^{air}	1, 415	Aspect	29.66	**<0.001**
	1, 415	Location	0.293	0.589
	1, 415	Aspect x location	0.490	0.484
T_{sum}^{air}	1, 415	Aspect	0.225	0.636
	1, 415	Location	10.467	**0.001**
	1, 415	Aspect x location	4.971	**0.026**
T_{range}^{air}	1, 425	Aspect	0.180	0.666
	1, 425	Location	24.79	**<0.001**
	1, 425	Aspect x location	22.12	**<0.001**

Table 2. The output of linear mixed models to determine the effect of leaf temperature parameters (T_{time}^{leaf}, T_{sum}^{leaf}, and T_{range}^{leaf}; Figure 2) on photosystem heat thresholds (T_{crit}). Bolded p-values indicate significance at a = 0.05.

Leaf temperature parameter	**df**	**F**	**p-value**
T_{time}^{leaf}	1, 33	0.129	0.72
T_{sum}^{leaf}	1, 27	4.478	**0.04**
T_{range}^{leaf}	1, 20	0.527	0.47

Figure 2. a) Variation in heat tolerance thresholds (T_{crit}) across five days of sampling in summer (26 Feb – 2 Mar). Letters represent significant differences in T_{crit} between days of sampling. Error bars show the standard error of mean T_{crit}. All daily T^{leaf} parameter values were averaged across the week of leaf temperatures leading up to and coinciding with T_{crit} sampling (22 Feb – 28 Feb). b) The relationship between average time of maximum temperature (T_{time}^{leaf}) and T_{crit}. c) The relationship between average daily heat sum (T_{sum}^{leaf}) and T_{crit}. d) The relationship between average diurnal temperature range (T_{range}^{air}) and T_{crit}. Solid lines represent statistically significant relationships, and dashed lines represent non-significant relationships from linear mixed models; conditional R^2 values are shown above their corresponding relationship.

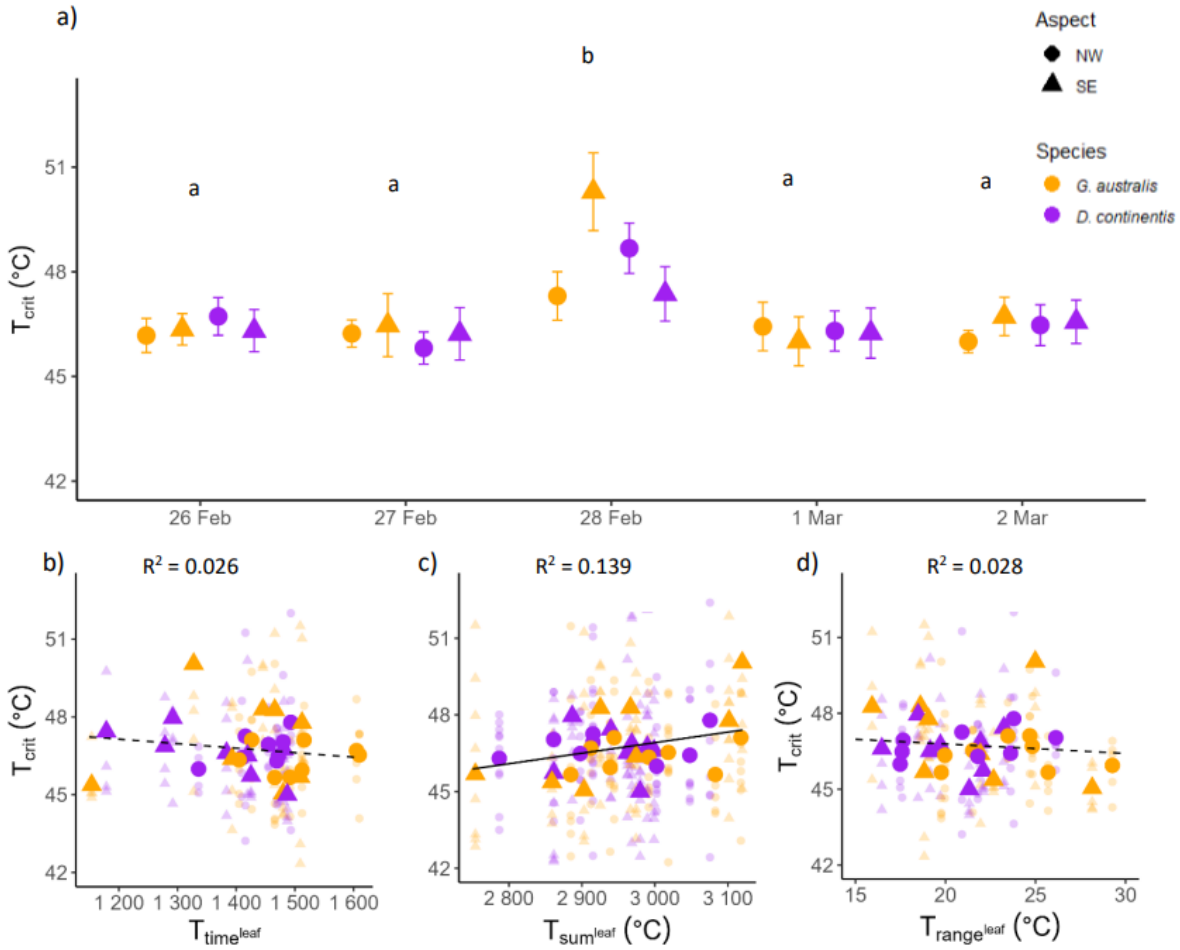

Figure 3. Snap Boosting Machine Regressor model for predicting the effects of the historical leaf temperature profiles on heat tolerance thresholds (T_{crit}) based on leaf temperatures averaged across two species and 16 sites recorded at 5-minute intervals (1,152 time points per day of T_{crit} measurement). The data shown represent the leaf temperature profile within the four days preceding each of the five days of T_{crit} measurement. Because T_{crit} was measured on five consecutive days, a given time point prior to T_{crit} measurement represented five sets of species-site combinations (32 plants per day totalling to 36,864 leaf temperatures for each day of T_{crit} measurement, Figure S6). (a) Leaf temperature (°C) over the four-days, with individual timepoints shown in dark grey and the light grey shadow indicating the standard deviation for each time point. Machine learning (ML) predictive features are the 33 points highlighted in colours representing their temperature, with blue indicating lower and red indicating higher leaf temperatures. The ML predictive points indicate the times at which leaf temperature had the highest predictive power for T_{crit} measured. (b) The individual predictive power of each of the 33 ML features, with the total predictive power of all points taken together explaining 84.9% of the variation in T_{crit}, with three temperature points having between 10-15% predictive power each (marked with grey ellipses).

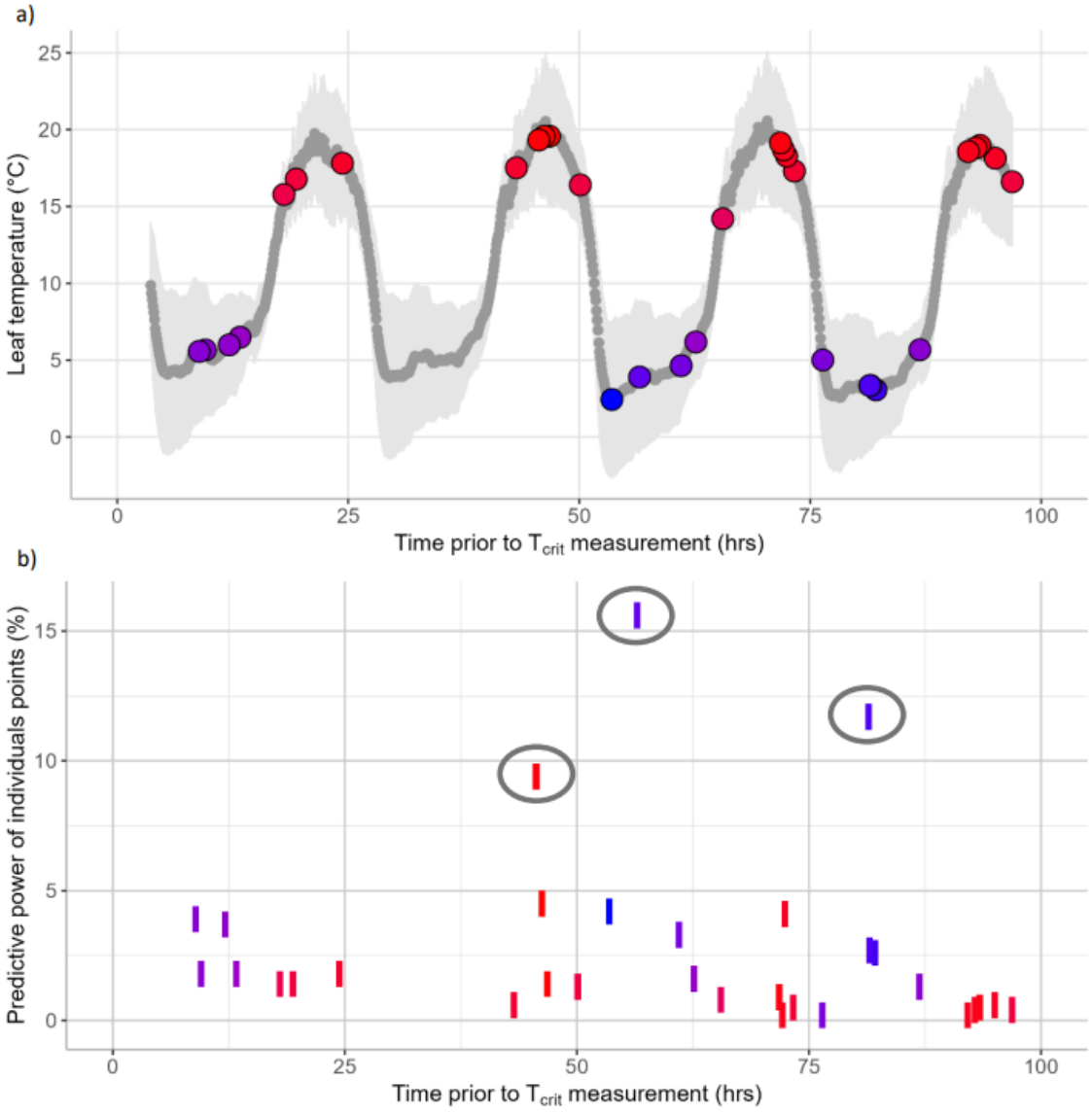

Supplementary Materials

Supporting Information 1. Selection of sites contrasting in aspect.

Selection for each site pair was based on four criteria: 1) whether sites were reasonably matched in elevation (within 10 m), 2) whether their aspects were contrasting (North-West facing vs South-East facing), and 3) whether the distance between the target *G. australis* and *D. continentis* plants was more than 1 m apart. The latter criterion was to ensure that thermocouples were run only a short distance to the datalogger and that microclimatic conditions that the plants were exposed to were comparable.

12

Table S1. Coordinates, elevation, slope and aspect of study microsites across Schlink Pass and Mt Stilwell in Kosciuszko National Park of South-East New South Wales. Latitude and longitude values are formatted in decimal degrees. The nomenclature of the site names are as follows: the first two letters, 'Sp' and 'St' represent the site location, Schlink Pass and Stilwell, respectively and the last two letters of each abbreviated site name represent the aspect of the site. Although not all sites were directly NW/SE facing, a LMM where date was a random factor revealed highly significant variation in mean air temperatures between sites of opposing aspects across the year 2023 ($p < 0.001$, Bird et al., unpublished data). This justified the grouping of paired sites into NW and SE categories.

Site	**Latitude**	**Longitude**	**Elevation (m a.s.l)**	**Aspect**	**Slope**
Stilwell					
St1SE	-36.44111	148.3239	1962	SE 175 °	5 °
St1NW	-36.44111	148.3225	1953	NW 300 °	15 °
St2SE	-36.44778	148.3322	1959	SE 125 °	10 °
St2NW	-36.44222	148.3264	1960	NW 332 °	10 °
St3SE	-36.44583	148.3328	1952	SE 117 °	5 °
St3NW	-36.44194	148.3278	1963	NW 322 °	10 °
St4SE	-36.44472	148.3344	1956	NE 27 °	15 °
St4NW	-36.4428	148.3297	1963	NW 322 °	10 °
Schlink Pass					
Sp1SE	-36.26444	148.3731	1690	E 120 °	25 °
Sp1NW	-36.26477	148.3733	1680	NW 330 °	10 °
Sp2SE	-36.26694	148.3714	1672	E 70 °	20 °
Sp2NW	-36.26719	148.3719	1672	W 270 °	5 °
Sp3SE	-36.26806	148.3711	1667	E 90 °	20 °
Sp3NW	-36.26843	148.3718	1660	SW 240 °	15 °
Sp4SE	-36.26861	148.3708	1665	SE 150 °	5 °
Sp4NW	-36.26889	148.3708	1664	NW 300 °	5 °

13
14

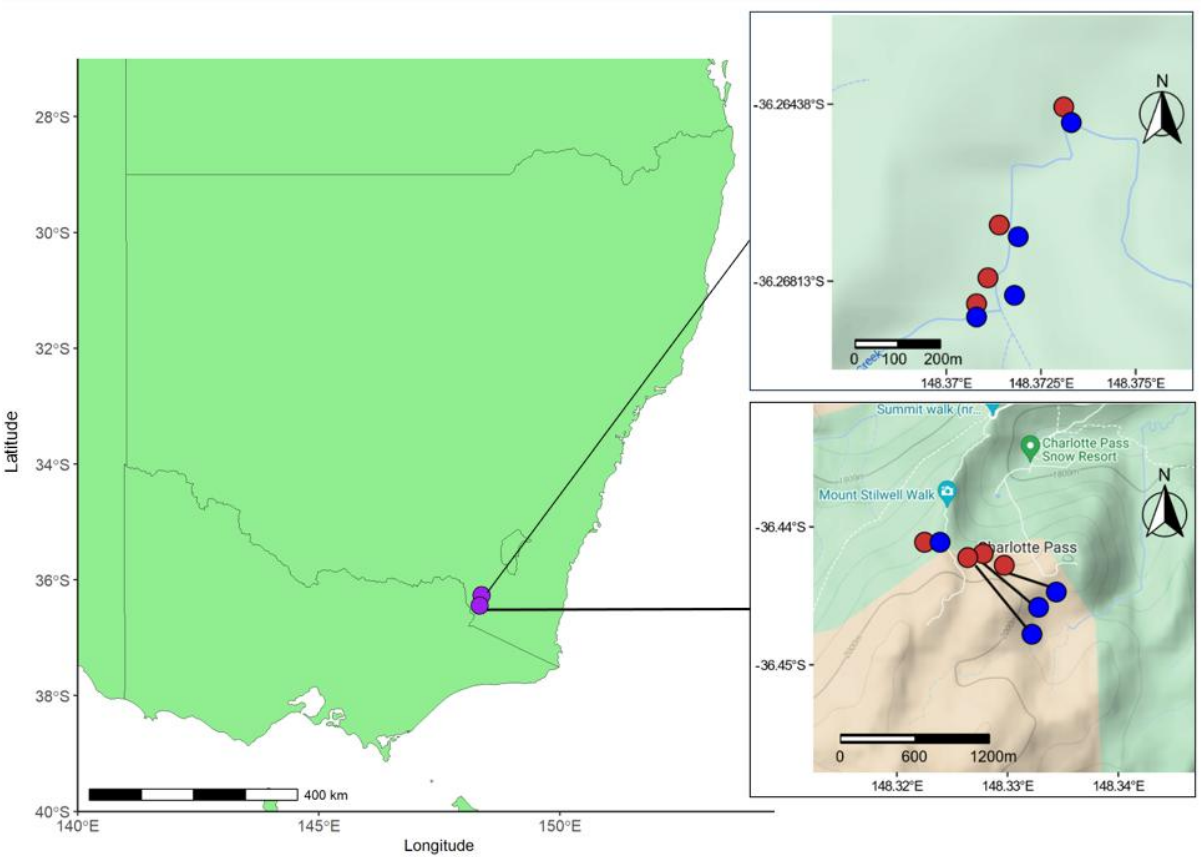

Figure S1: Sixteen study sites throughout Schlink Pass (top) and Mt Stilwell (bottom) in South-Eastern Australia on topographic maps. Red circles indicate N-NW facing sites; blue circles indicate S-SE facing sites. At each location, there were four site pairs, each pair matched in elevation but contrasted in aspect. Thin black lines indicate which sites are paired where unclear. Scale bars and north arrows are on each map. The map products were generated using the *"ggmap"* (Kahle & Wickham, 2013) and "*ggplot2"* (Wickham, 2016) R packages.

15

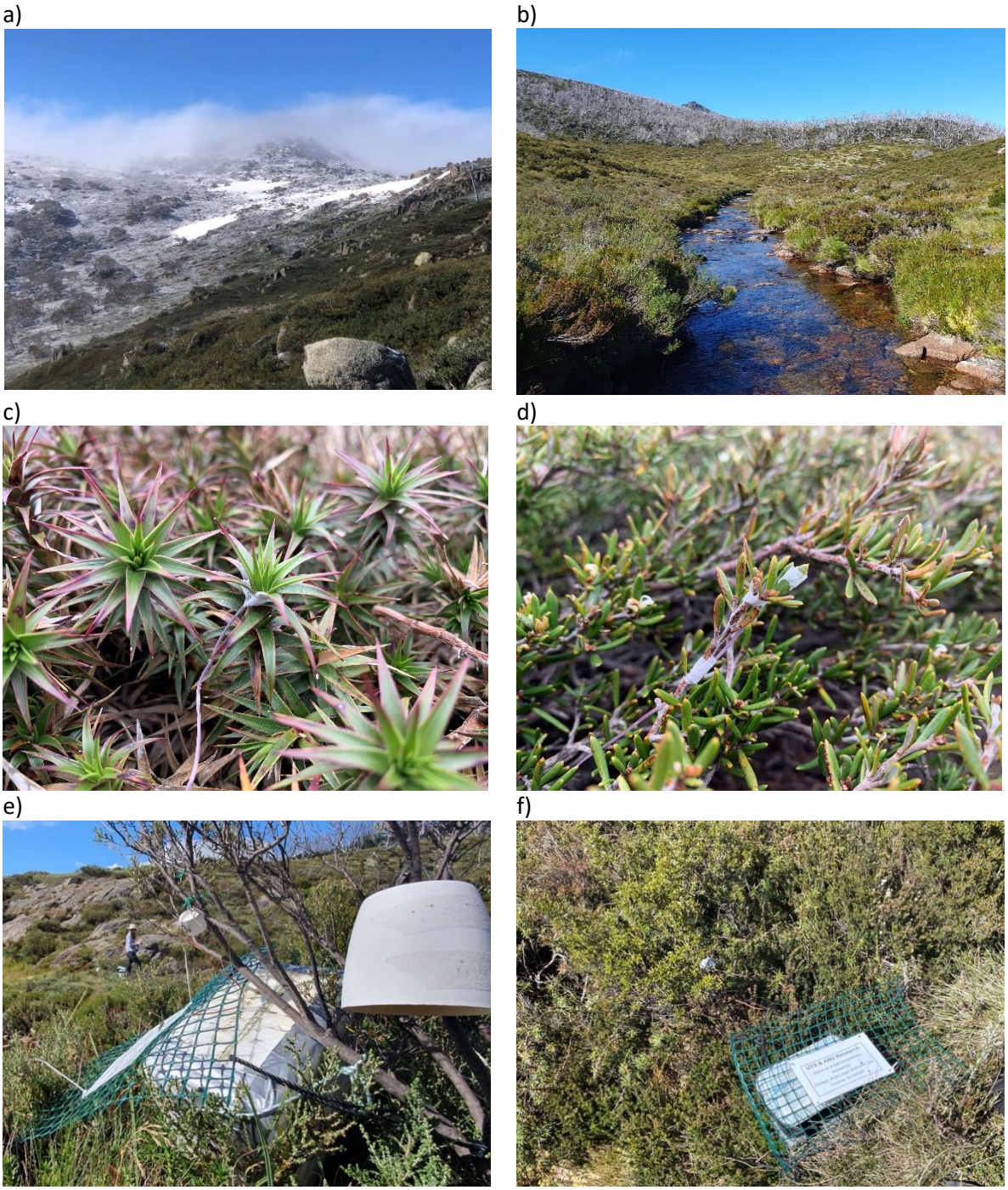

Figure S2. In-field setup of temperature logging stations at study microsites in Kosciuszko National Park, New South Wales across two locations: a) Mount Stilwell and b) Schlink Pass. Thermocouples recording leaf temperature of c) D*. continentis* and d) *G. australis.* e) A Thermocouple recording air temperature protected by a white cap. f) Thermocouples were connected to dataloggers an kept in a waterproof esky, protected using plastic garden netting.

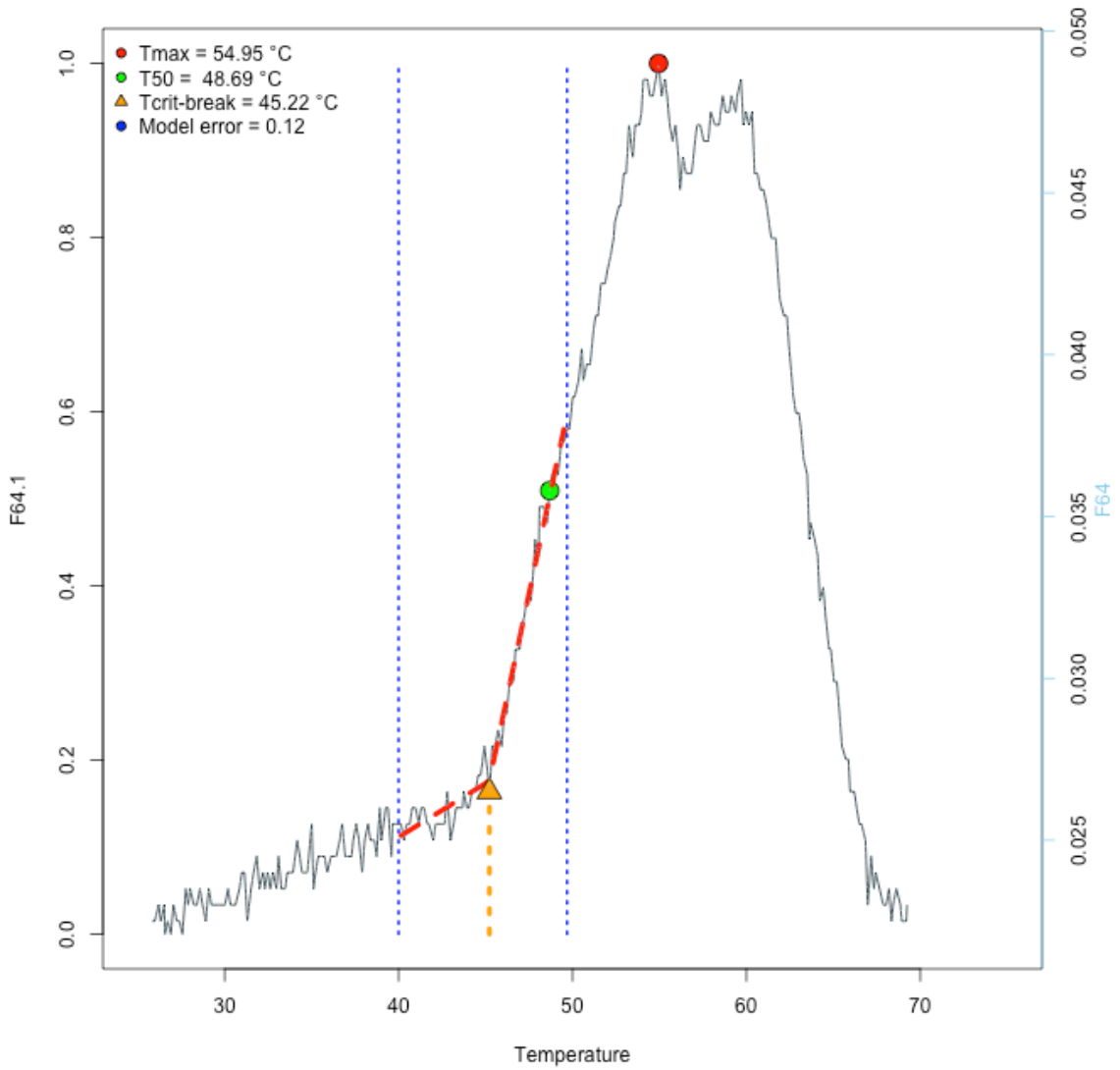

Figure S3. An example of a chlorophyll-fluorescence curve (T-F_o). The curve shows an increase in baseline chlorophyll fluorescence with an increase in temperature. The triangle indicates the T_{crit} threshold.

Table S2. Average maximum and minimum air temperatures, T_{time}^{air}, T_{sum}^{air} and T_{range}^{air} for NW and SE aspects at both study locations. Values for each variable were averaged across the four replicates for each site type and the 28 days of February 2023.

Location	Aspect	Mean maximum air temperature (°C)	Mean minimum air temperature (°C)	T_{time}^{air} (hrs)	T_{sum}^{air} (°C)	T_{range}^{air} (°C)
Schlink Pass	NW	22.5 ± 0.5	0.86 ± 0.3	15.1 ± 0.2	3269 ± 93	22.3 ± 0.7
	SE	24.9 ± 0.6	0.4 ± 0.3	13.7 ± 0.2	3373 ± 101	23.0 ± 0.6
Mt Stilwell	NW	24.3 ± 0.8	3.1 ± 0.3	15.1 ± 0.4	3208 ± 108	21.3 ± 0.8
	SE	20.6 ± 0.9	3.1 ± 0.3	13.3 ± 0.4	3047 ± 128	17.5 ± 0.9

20

Table S3. The output of linear mixed models to determine the influence of aspect (NW v SE) and location (Schlink Pass v Mt Stilwell) on site-specific daily heat sum (T_{sum}^{air}), time of day that maximum temperatures were reached (T_{time}^{air}) and diurnal temperature range (T_{range}^{air}) across the month of February 2023.The model included the sampling date as a random factor to account for variation in heat sum caused by differences in weather across days (Figure S5). Bolded p-values indicate significance at $\alpha = 0.05$.

Response variable	df	Explanatory variables	F	p-value
T_{time}^{air}	1, 415	Aspect	29.66	**<0.001**
	1, 415	Location	0.293	0.589
	1, 415	Aspect x location	0.490	0.484
T_{sum}^{air}	1, 415	Aspect	0.225	0.636
	1, 415	Location	10.467	**0.001**
	1, 415	Aspect x location	4.971	**0.026**
T_{range}^{air}	1, 425	Aspect	0.180	0.666
	1, 425	Location	24.79	**<0.001**
	1, 425	Aspect x location	22.12	**<0.001**

Table S4. The output of linear mixed models to determine the effect of leaf temperature parameters ($T_{sum\text{-}day}^{leaf}$, and $T_{sum\text{-}night}^{leaf}$; Figure 2) on photosystem heat thresholds (T_{crit}).

Leaf temperature parameter	**df**	**F**	**p-value**
$T_{sum\text{-}day}^{leaf}$	1, 27	3.07	0.99
$T_{sum\text{-}night}^{leaf}$	1, 27	3.1	0.09

Figure S4. RWC for *G. australis* and *D. continentis* at the four site-types (SchlinkSE, SchlinkNW, StilwellNW, StilwellSE). All data were collected between the 25 Feb and 1 March 2023, overlapping with the T_{crit} sampling period.

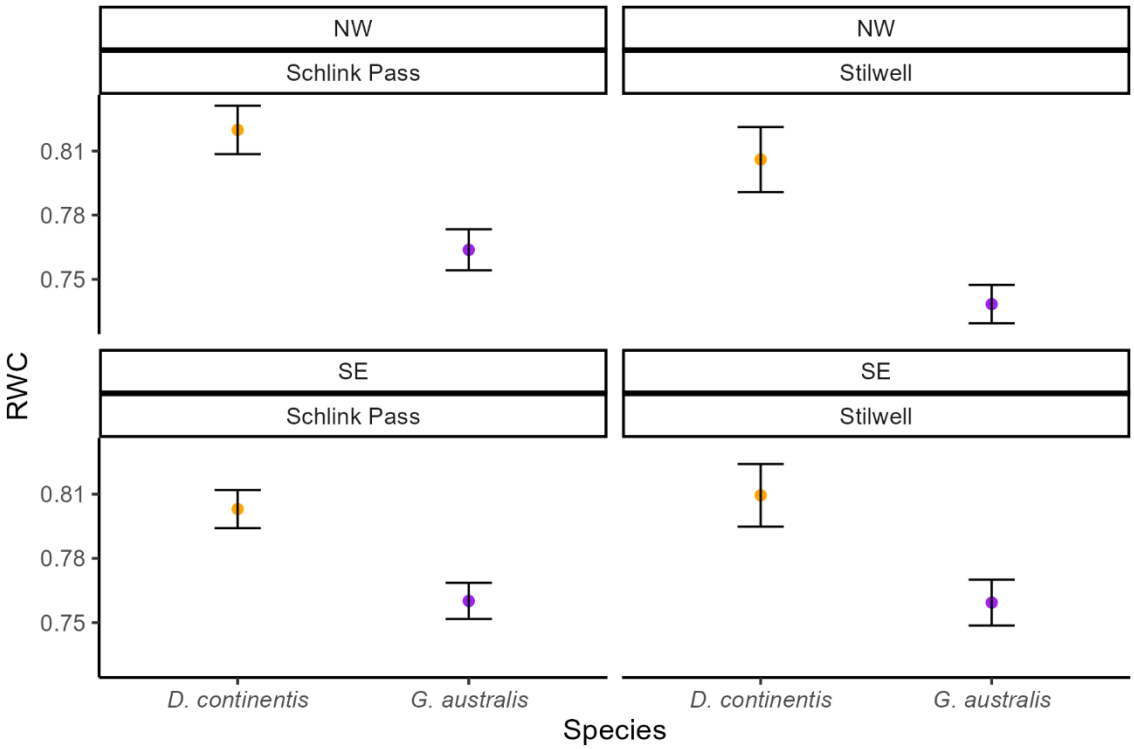

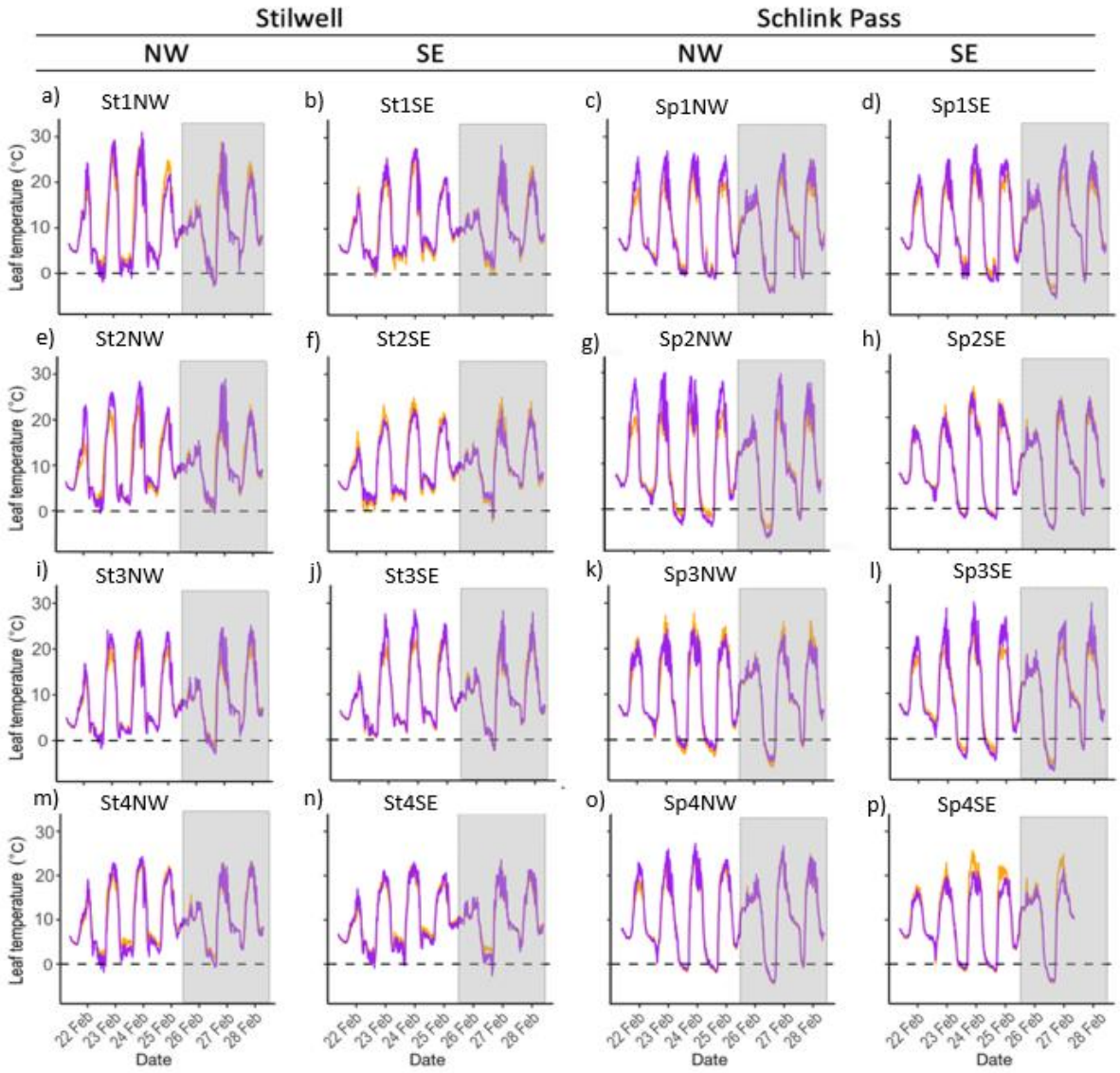

Figure S5. Leaf temperatures (°C) of *Dracophyllum continentis* (purple lines) *and Grevillea australis* (yellow lines) across seven days (22–28 Feb) leading up to and coinciding with T_{crit} sampling (26 Feb–2 Mar). Leaf temperatures were measured in situ at 16 sites across two alpine locations (Schlink Pass and Mt Stilwell) that contrasted in aspect (SW v NE). Tick marks on the *x*-axis align with data recorded at 3 pm on that day. The dashed horizontal lines represent 0°C, and the grey shading represents the first three days of T_{crit} sampling.

22 Feb	23 Feb	24 Feb	25 Feb	26 Feb	28 Feb	1 Mar	2 Mar	Time points	Leaf temperature points
			T_{crit}	T_{crit}	T_{crit}	T_{crit}	T_{crit}		
288	288	288	288					1152	36864
	288	288	288	288				1152	36864
		288	288	288	288			1152	36864
			288	288	288	288		1152	36864
				288	288	288	288	1152	36864
288	576	864	1552	1152	864	576	288	5760	184320

Figure S6. Number of time points and leaf temperatures included in the SnapBoosting Machine Regressor model used to predict the effects of historical leaf temperature profiles on heat tolerance thresholds (T_{crit}). Time points for each four-day period preceding a day of T_{crit} measurements are shown in rows 3–7. The darkest shade represents time points within the 24 hours preceding each day of T_{crit} measurement, while the lightest shade represents time points 72–96 hours prior. Each time point corresponds to 32 unique leaf temperature measurements (recorded from two species across 16 sites). In total, 1,552 time points and 36,864 unique leaf temperature values were used to predict the 32 T_{crit} values for each measurement day. Across all 32 plants and all five T_{crit} measurement days, a total of 5,670 time points and 184,320 leaf temperature values were used to predict T_{crit} in this four-day model.

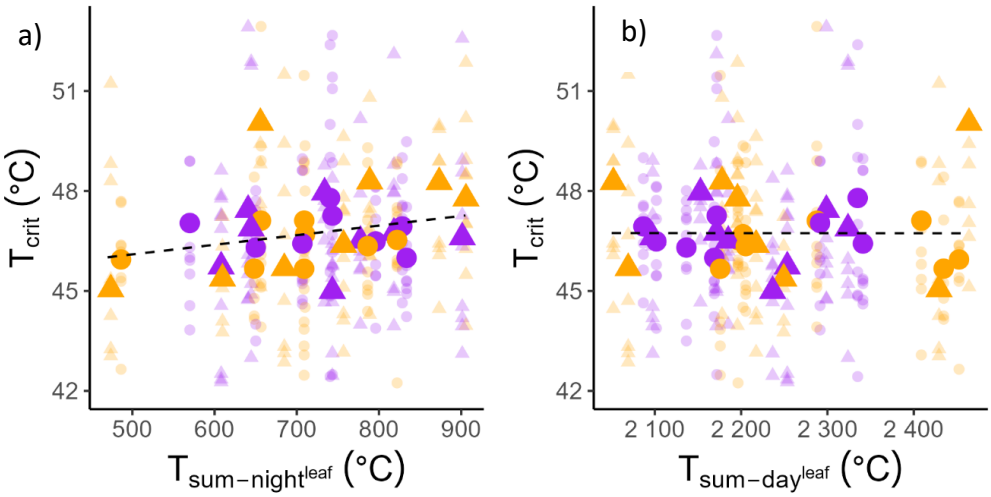

Figure S7. Daily T^{leaf} parameters values were averaged across the week of leaf temperatures leading up to and coinciding with T_{crit} sampling (22 Feb – 28 Feb). a) The relationship between average day time heat sum ($T_{sum\text{-}night}^{leaf}$) and T_{crit}. b) The relationship between average day time heat sum ($T_{sum\text{-}night}^{leaf}$) and T_{crit}. Dashed lines represent non-significant relationships from linear mixed models.

Bird, M., Pottinger, C., Arnold, P., Danzey, L., Geange, S., Kearney, M., . . . Leigh, A. (unpublished data). Can NicheMapR predict leaf temperatures of morphologically disparate species across microclimatically distinct alpine sites?

Kahle, D., & Wickham, H. (2013). ggmap: Spatial Visualization with ggplot2. *The R Journal, 5*(1), 144-161.

Leon-Garcia, I. V., & Lasso, E. (2019). High heat tolerance in plants from the Andean highlands: Implications for paramos in a warmer world. *PLoS One, 14*(11), e0224218. doi:10.1371/journal.pone.0224218

Wickham, H. (2016). *ggplot2: Elegant Graphics for Data Analysis*: Springer-Verlag New York.